A New Strategy for the Design of Water-Soluble Synthetic Receptors: Specific Recognition of DNA Intercalators and Diamines.

Kenji Wada,[a] Tadashi Mizutani,*[a,c] Hideki Matsuoka,[b] and Susumu Kitagawa[a]

Abstract: Water-soluble zinc bisporphyrin receptors **1** and **2** having two Lewis acidic sites (zinc) in the hydrophobic environment consisting of alkyl chains and a bisporphyrin framework, and covered with hydrophilic exterior (twelve or eighteen carboxyl groups) were prepared. The receptors show high affinity for diamines and DNA intercalators in water where the binding constants K_a are of the order of 10^7 and $10^8\,\text{M}^{-1}$, respectively. Diamines and DNA intercalators are bound to the receptor through different mechanisms. Diamines are bound through hydrophobic interactions and zinc–nitrogen interactions, while DNA intercalators are bound through hydrophobic interactions and charge-transfer interactions. Flexible alkyl chains can make van der Waals contact with guests and create a hydrophobic environment around the bound guest by an induced-fit-type mechanism. For the binding of DNA intercalators, the following features are noteworthy: 1) Binding constants are similar between the zinc porphyrins and zinc-free porphyrins; 2) the binding constant is larger for the guest having the lower LUMO; this indicates the important contribution of charge-transfer interactions to binding; 3) the hydrophobic and cationic nature of DNA intercalators is substantially important, and 4) higher ionic strength reduced the binding affinities; this shows a moderate contribution of electrostatic interactions. The conformational instability of the receptors also contributes to the tight binding: hydrophobic and electrostatic interactions cannot both be favorable at the same time in the guest-free receptor. Enthalpy–entropy compensation observed for the binding of diamines and DNA intercalators is characterized by a relatively small slope ($\alpha = 0.74$) and a large intercept ($\beta = 7.75\,\text{kcal mol}^{-1}$) in the ΔH° versus $T\Delta S^\circ$ plot; this shows that a conformational change of receptors and a significant desolvation occur upon binding. The receptor can competitively bind to propidium iodide to deprive DNA of the intercalated propidium iodide. These features of water-soluble receptors consisting of a rigid framework and flexible side chains with a large solvent-accessible area are in contrast to highly preorganized rigid receptors, and they can provide useful guidelines for rational design of induced-fit artificial receptors in water.

Keywords: hydrophobic interaction · induced-fit binding · molecular recognition · porphyrinoids · receptors

Introduction

Considerable efforts in host–guest chemistry have been devoted to the design of artificial water-soluble receptors with high binding affinity comparable to that of proteins.[1–5] Kuntz et al.[6] investigated the binding constants of various guests to proteins as a function of the size of the guests, and showed that the binding constants increase with increasing guest size and reach saturation at about $10^{9.3}\,\text{M}^{-1}$. On the other hand, synthetic receptors show much smaller binding constants when compared with proteins. For instance, cyclodextrins bind hydrophobic guests such as substituted benzenes with association constants ranging from 10^2–$10^4\,\text{M}^{-1}$, thus proteins bind ligands 10^5–10^7 times more strongly.[7] In artificial receptor chemistry, a breakthrough to overcome this gap has been intensively sought. To our knowledge there are only a few examples of synthetic receptors with a binding affinity similar to natural receptors. Lehn et al.[8] demonstrated that the macrocyclic receptor composed of a polyammonium moiety and an acridine side-chain bound tightly to ATP ($K_a = 10^{11}\,\text{M}^{-1}$) and catalyzed its hydrolysis reactions, here ionic or polar interactions between the receptor and guests effectively stabilize the complex. Breslow et al.[9] reported that the doubly linked β-cyclodextrin dimer binds strongly to ditopic substrates in water ($10^{10}\,\text{M}^{-1}$). The origin of this high

[a] Prof. Dr. T. Mizutani, Dr. K. Wada, Prof. Dr. S. Kitagawa
Department of Synthetic Chemistry and Biological Chemistry
Graduate School of Engineering, Kyoto University
Sakyo-ku, Kyoto 606-8501 (Japan)

[b] Prof. Dr. H. Matsuoka
Department of Polymer Chemistry
Graduate School of Engineering, Kyoto University
Sakyo-ku, Kyoto 606-8501 (Japan)
Fax: (+81) 75-753-5609

[c] Current address:
Department of Molecular Science and Technology
Faculty of Engineering, Doshisha University
Kyotanabe, Kyoto 610-0321 (Japan)
Fax: (+81) 774-65-6803
E-mail: mizu_tad@yahoo.co.jp

DOI: 10.1002/chem.200204481

affinity is ascribed to the geometrical optimization of hydrophobic interactions and van der Waals interactions. Apparently, the strategy for guest design is based on the preorganization principle: highly preorganized receptors having a rigid framework such as aromatic groups or a cyclic structure show minimal conformational reorganization upon binding, leading to tight binding.[10] This preorganization strategy has been successfully applied to receptors targeting relatively small guests. We should note that, when the target guest is larger and has larger molecular surface, preorganization is especially difficult due to the complicated fabrication of the receptor–ligand complementary interface and the many obstacles in synthetic routes to receptors.

A number of studies from the biological[11–12] and chemical[13–15] points of view have suggested that a larger receptor–guest contact surface area would result in a greater driving force from receptor–guest interactions and solvent reorganization. To design a receptor having a large interfacial area, a new strategy should be developed. Our strategy for the design of artificial receptors is to use both a rigid scaffold and flexible side chains to construct a binding pocket encompassing the guest. The advantages of using flexible side chains are twofold. First, they can make contact with the guest through a wide surface area to have large van der Waals stabilization energy as well as large desolvation entropic gain.[12, 15] Second, synthetic difficulties for the preorganized structure can be partly avoided since the side chains can induced-fit[16] to the shape of the guest. Another point, which might be important for the receptor design, is to append polar recognition groups to the hydrophobic binding pocket. We can expect that the polar interaction in the nonpolar microenvironment would operate effectively to drive the host–guest complex formation.

We report here the synthesis and guest-binding properties of bisporphyrins designed by using this strategy. Porphyrins are known as one of the most versatile receptor scaffolds, because 1) there are systematic and comprehensive studies on their synthesis; 2) they have high susceptibility for various spectroscopic methods; and 3) they have a hydrophobic surface area of 7×7 Å^2, all of which are very attractive properties for water-soluble receptors. Systematic studies here clarified the importance of control of a variety of interactions, such as hydrophobic interactions, van der Waals interactions, electrostatic interactions, coordination interactions, and charge-transfer interactions. Special emphasis is placed on conformational reorganization of the receptors and its implication for binding energetics in water.

Results and Discussion

Design and synthesis of bisporphyrin receptors: We designed synthetic receptor molecules that meet the following requirements: 1) The molecule has enough hydrophilic groups on its surface to have sufficient solubility in water. 2) It has hydrophobic groups inside the molecule, constructing a hydrophobic binding pocket for guest accommodation. 3) In the hydrophobic pocket, there are polar recognition groups for guest selectivity. The designed receptors **1** and **2** have a dimeric-porphyrin structure combined at the *meso* position with a *m*-phenylene spacer, which is commonly referred to as a gable framework,[17] and exhibit tight binding to diamines in organic solvent due to the strictly fixed geometry of two Lewis acidic centers at a distance of 11 Å.[18] In our receptors **1** and **2**, as well as monomeric analogue **3**,[19] ω-carboxyalkoxy groups are introduced at the two *ortho* positions of the phenyl groups; this gives spatial confinements around the metal centers and the porphyrin plane. The alkyl moieties are capable of making a hydrophobic environment together with the rigid gable porphyrin framework. Twelve or eighteen carboxyl groups form a hydrophilic exterior that imparts sufficient water solubility of receptors at neutral to basic pH. The zinc ions and highly polarizable porphyrins in the hydrophobic binding pocket are expected to serve as an additional driving force of binding such as coordinative interactions and charge-transfer interactions. Receptor **1** has twelve carboxyalkoxy groups and receptor **2** has eight carboxyalkoxy groups. Comparison of binding affinity between the two receptors would clarify the importance of flexible alkoxy groups for binding. The free base **1**·H_2 was prepared to probe the role of zinc in binding.

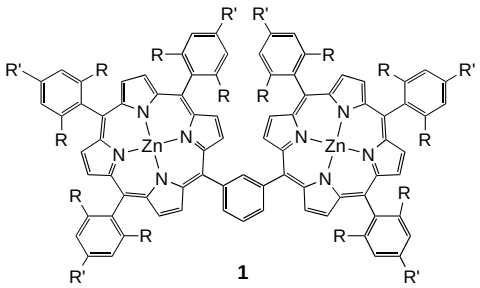

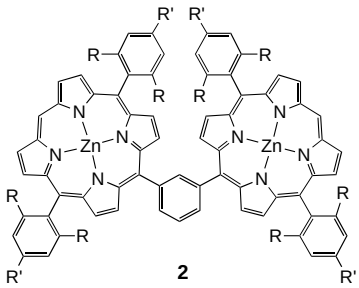

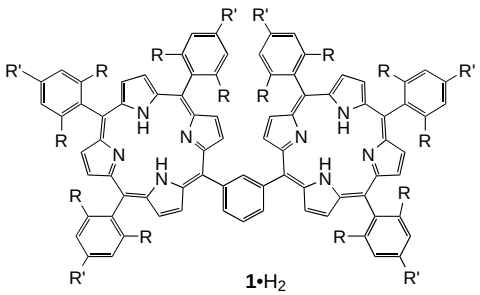

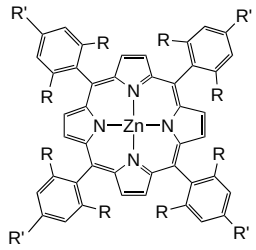

We employed a novel synthetic route to the gable porphyrins (Scheme 1) for versatile preparation of analogues

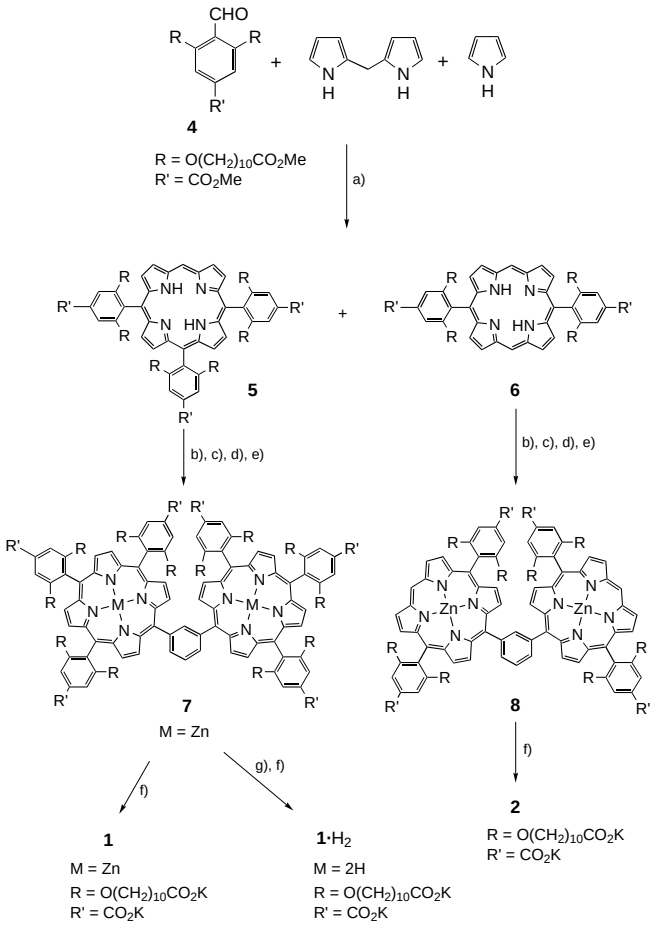

Scheme 1. Synthesis of receptors **1**, **2**, and **1**·H_2: a) TFA/CH_2Cl_2, then DDQ; b) $Zn(OAc)_2$/$CHCl_3$; c) NBS/$CHCl_3$, py; d) $PdCl_2(PPh_3)_2$, pinacolborane, TEA/$ClCH_2CH_2Cl$; e) 1,3-diiodobenzene, $Pd(PPh_3)_4$, Cs_2CO_3/DMF; f) KOH/MeOH-THF (0.5 M); g) HCl (5 M).

of highly functionalized bisporphyrins. The route was quite different from that reported by Tabushi et al.[17] and enabled us to synthesize the porphyrins in a fewer steps. Two monomeric porphyrins (A_3B-type **5** and *trans*-type **6**) were prepared by Lindsey's method[20] from aldehyde **4**, dipyrromethane and pyrrole, by using trifluoroacetic acid as an acid catalyst, followed by chromatographic separation. After zinc insertion, each porphyrin was monobrominated[21] at the *meso* position by *N*-bromosuccinimide, and a subsequent reaction with pinacolborane yielded *meso*-substituted porphyrylboronate.[22] Dimerization of the two porphyrins was achieved by the Suzuki cross-coupling reaction.[23] In this reaction it was particularly important to properly select solvent and base; the reaction did not proceed when the bases triethylamine, pyridine, KF, K_2CO_3, Na_2CO_3, $Ba(OH)_2$, NaOMe, LiOMe, and the solvents THF, benzene, toluene, CH_2Cl_2, were used. The reaction conditions were optimized and found to be a Cs_2CO_3/anhydrous DMF system. Finally alkaline hydrolysis of all the ester groups of **7** and **8** afforded the water-soluble gable porphyrins **1** and **2**, respectively. The free base of **1**, **1**·H_2, was prepared by quantitative demetallation of **7** with HCl, followed by alkaline hydrolysis.

Receptors **1** and **2** are soluble in polar solvents such as water and methanol. In the ^{1}H NMR spectra of **1** and **2** ([receptor] = 1.5 mM) in deuterated borate buffer (I = 100 mM, pD 8.6) at 25 °C, all signals were broad; this indicates that receptors are aggregated at the millimolar concentration. When the temperature was raised to 80 °C, the proton signals of **2** became partly sharp whereas those of **1** remained broad. Bisporphyrin **1**, therefore, has a stronger tendency to form aggregates in water. High-resolution NMR spectra were obtained in deuterated methanol (Figure 1). As would be

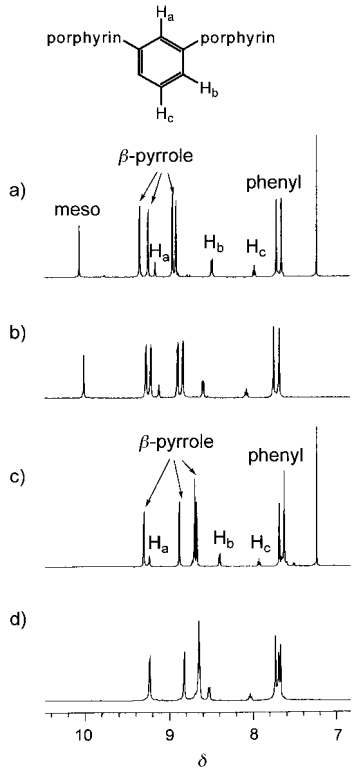

Figure 1. ^{1}H NMR spectra of porphyrin receptors **1**, **2**, **7**, and **8** in the downfield region at 25 °C. a) **8** in $CDCl_3$; b) **2** in CD_3OD; c) **7** in $CDCl_3$; d) **1** in CD_3OD.

expected, the signal of H_a on the benzene spacer underwent remarkable downfield shifts (9.24 ppm for **7** and 9.17 ppm for **8**) due to the diamagnetic anisotropy of the ring current of the gable porphyrin. Pyrrole protons of **7** and **1** were observed as two doublets (at $\delta = 9.31$ and 8.90 for **7**, $\delta = 9.24$ and 8.83 for **1**) and one AB quartet ($\delta = 8.70$ for **7** and 8.65 for **1**), the same splitting pattern as that of 1,3-bis(*meso*-triphenylporphinyl)-benzene.[17] Proton signals from the *ortho*-substituted phenyl groups of **2** were observed as two singlets ($\delta = 7.66$ and 7.72), corresponding to one at the gabled inner space and the other at the outer space. Rotation about all the porphyrin – benzene bonds is therefore restricted at room temperature.

Analysis by small-angle X-ray scattering on a solution of **2** (740 μM) in borate buffer (I = 100 mM, pH 9.0) at 25 °C gave an estimate of the particle radius of 15 Å, which is in good agreement with that of the discrete molecule. No micellar-like aggregate was formed. The absorbance in the Q-band obeyed the Lambert – Beer law up to at least 90 μM in borate buffer (I = 100 mM, pH 9.0) at 25 °C, indicating that the porphyrins in the micromolar concentration are monomeric. At pH < 7.5, a gradual decrease in the absorbance in the Soret band was

observed; this suggests that partial protonation of the carboxylate groups induced aggregation of the bisporphyrin. Thus, the binding experiments were performed at pH 8 or 9.

Binding of diamines: The binding of diamines was investigated by using UV-visible and fluorescence spectroscopic titration in borate buffer.[24] As shown in Figure 2, addition of the guest caused a red-shift in the Soret band, a typical

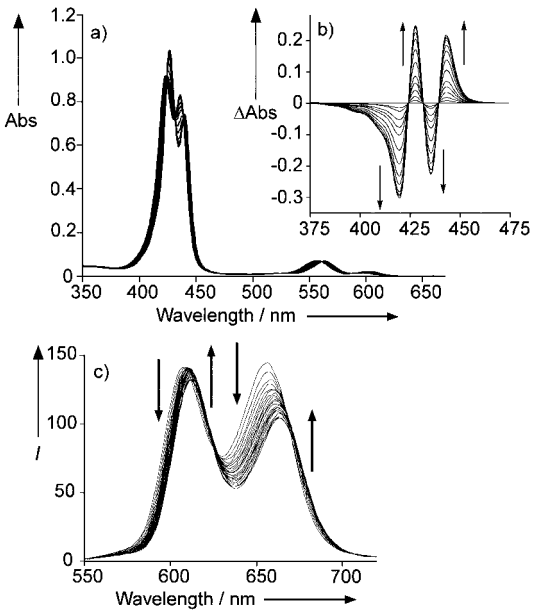

Figure 2. Spectral changes of **1** in borate buffer ($I = 100$ mM, pH 9.0) upon addition of 1,2-bis (4-pyridyl)ethane **G1** at 25 °C. a) UV/Vis spectra; $[\mathbf{1}]_0 =$ 1.7 μM, $[\mathbf{G1}]_0 = 0-4.70$ μM; b) difference spectra of (a); c) Fluorescence spectra; $[\mathbf{1}]_0 = 48$ nM, $[\mathbf{G1}]_0 = 0-662$ nM, excitation at 424 nm.

spectral change due to the amino group coordinating to zinc.[25] The split Soret band is characteristic of the *meta*-phenylenebis(porphyrin) framework, in which the angle between the two transition moments of porphyrins is 120°, resulting in two energetically inequivalent excited states.[26, 27] On the basis of the previous studies on complexation of diamines to zinc bisporphyrins,[28] the large magnitude of the binding constants, and the clearly observed isosbestic points, we concluded that guest forms a 1:1 complex with the porphyrin. The fluorescence emission of the porphyrin was also shifted to longer wavelength upon addition of diamines, without quenching of the fluorescence emission. The binding constants were determined by least-squares fitting of the absorbance changes at 420, 428, 436 and 443 nm or fluorescence intensity changes at 655 nm to the 1:1 binding isotherm. For **G1** and **G4**, the binding constants determined by fluorescence titration were in good agreement with those determined by UV-visible titration, although the typical concentration of porphyrins was 48 nM in the former and 1.7 μM in the latter experiments. The binding constants are listed in Table 1.

Free-base porphyrin $\mathbf{1}\cdot H_2$ did not bind all bidentate diamines (**G1**–**G4**); this indicates that zinc is essential in diamine binding. Tight binding of diamines to zinc bisporphyrin in organic solvents is reported in several studies.[28] The

Table 1. Binding constants, K_1 (upper value), K_2 (lower value), between porphyrin receptors and guests in borate buffer ($I = 100$ mM, pH 9.0) at 25 °C.[a]

guest	K_1 and K_2 [M^{-1}] **1**	**1**·H_2	**2**
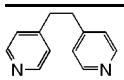 **G1**	3.7×10^7	n.b.[b]	3.1×10^5
G1[c]	1800	n.b.[b]	1100
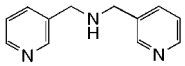 **G2**	5.13×10^6	n.b.[b]	1.7×10^5
His-His (**G3**)	610	n.b.[b]	320
His-Leu-His-β-NA[d] (**G4**)	1.2×10^6	n.b.[b]	1.4×10^5
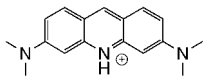 **G5**	2.8×10^8 5.1×10^7	1.8×10^8 5.6×10^7	2.1×10^{15}[e]
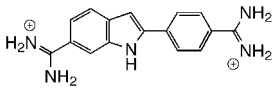 **G6**	3.0×10^6 2.2×10^6	2.9×10^6 6.4×10^6	1.1×10^{13}[e]
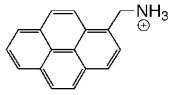 **G7**	1.0×10^7 1.1×10^7	1.1×10^6 2.1×10^6	1.7×10^{13}[e]
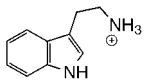 **G8**	3320 270	n.d.[f]	100 10
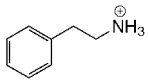 **G9**	760 180	n.d.[f]	130 30
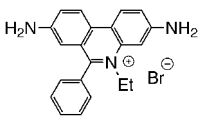 **G10**	2.5×10^8	7.2×10^6	7.0×10^6
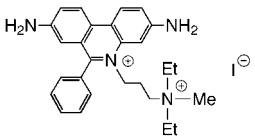 **G11**	2.7×10^8	1.2×10^7	2.5×10^6

[a] Binding constants are averages of 10–50 independent determinations. Estimated errors of the binding constant are less than 10%. UV/Vis spectroscopy was used for **G1**–**G4** and **G8**–**G9**, and fluorescence spectroscopy was used for **G5**–**G7** and **G10**–**G11**. [b] Not bound. [c] Binding constants were determined in MeOH/borate buffer 10:1 at 25 °C. [d] β-naphthylamido is abbreviated as β-NA. [e] Determined as K_1K_2. [f] Not determined.

high binding constants listed in Table 1 demonstrate that a similar strategy is applicable to diamine recognition in water.

The binding constant of **G1** to **1** was two orders of magnitude larger than that of **2**; this indicates the important role of ω-carboxyalkyl groups in the construction of a hydrophobic pocket for guest binding. The binding constant of **G1** was high in water ($\sim 10^7\,\text{M}^{-1}$) but low in methanol ($\sim 10^3\,\text{M}^{-1}$). These trends demonstrate that the strong binding in water should be ascribed to the hydrophobic interaction between the nonpolar moiety of **G1** and that of the receptors, and to the enhanced Lewis acid–Lewis base (Zn–nitrogen) interaction in the nonpolar environment. The low affinity of **G3** can be ascribed to the anion–anion electrostatic repulsion between its C-terminal carboxylate and the carboxylates of receptors. The binding constants for tripeptide **G4** were 2–3 orders of magnitude larger than those for **G3** because tripeptide **G4** has no negative carboxylate and has higher hydrophobicity due to the leucine side chain and the β-naphthyl group.

Since the detailed investigation of conformational changes of the alkyl chains by a ^{1}H NMR titration experiment in borate buffer failed due to aggregation of the receptors, we performed a ^{1}H NMR titration experiment in CD_2Cl_2 using dodecaester **8** and 1,2-bis(4-pyridyl)ethane **G1** ($K_a > 10^8\,\text{M}^{-1}$). The assignments of signals are based on ^{1}H–^{1}H COSY and homonuclear spin-decoupling experiments. As shown in Figure 3, addition of **G1** to a solution of porphyrin **8** caused the complexation-induced shifts of the proton resonances on the alkyl chains: a downfield shift of the methyl protons of the ester groups, H10′ and H9′, and an upfield shift of the methylene protons H1′ and H2′. Almost no changes in the corresponding proton resonances (Me2, H10, H9, H2 and H1) on the opposite side of the phenyl ring were observed. This suggests the following conformational changes, the C1′ and C2′ carbons move toward the porphyrin framework, and Me2′, C10′, and C9′ carbons are forced to move away from the porphyrin framework. It is interesting to note that the induced fit of the alkyl groups occurs even in organic solvent, and these observations suggest that similar induced fits occur more favorably in water owing to the hydrophobic interactions. In our previous studies,[19] similar guest-induced conformational changes were found for the binding of pyridine derivatives to a monomeric analogue **3** in water. All of these observations imply that similar conformational changes of **1** and **2** occurred during guest binding to accommodate nonpolar binding environment for the guest in water.

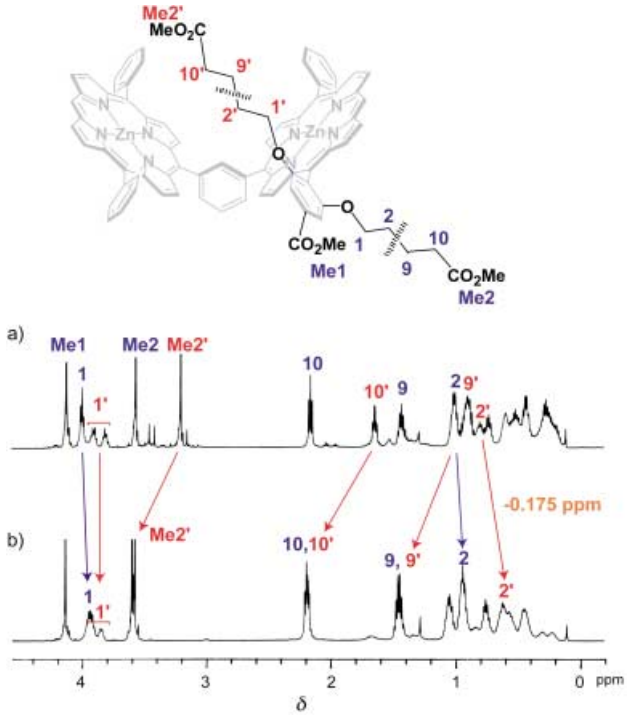

Figure 3. ^{1}H NMR spectra of gable porphyrin dodecaester **8** in the downfield region in $CDCl_3$ at 25 °C. a) **8** (1 mM); b) **8** and **G1** (both 1 mM).

Binding of DNA intercalators: Receptors bind more tightly to hydrophobic cations such as DNA intercalators[29] in borate buffer.[30] As shown in Figure 4, UV-visible spectra exhibit a red-shift of the Soret band upon addition of acridine orange

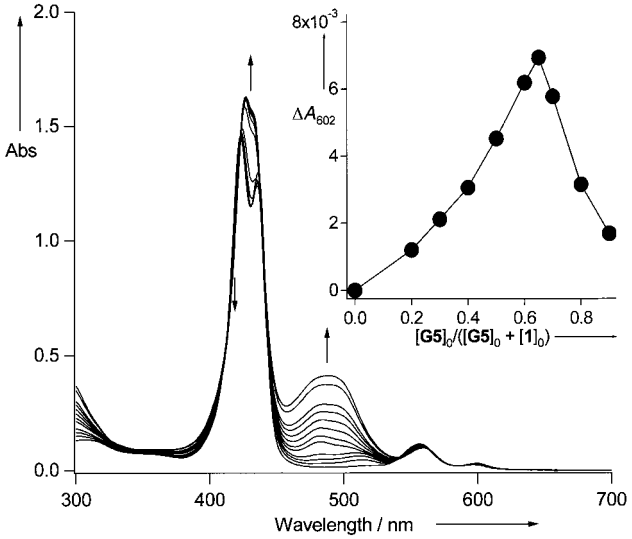

Figure 4. UV/Vis spectra of gable porphyrin **1** ($[\mathbf{1}]_0 = 2.4\,\mu\text{M}$) titrated with acridine orange base **G5** ($[\mathbf{G5}]_0 = 0$–$11.6\,\mu\text{M}$) in borate buffer ($I = 100$ mM, pH 9.0) at 25 °C. Inset: the Job plot at 602 nm, the total concentration ($[\mathbf{1}]_0 + [\mathbf{G5}]_0$) is 8.7 μM.

base (**G5**), and the inflection point on the Job plot was observed at 0.66. The fluorescence emission of **G5** was completely quenched when the molar ratio of **G5** to **1** is less than 2 (Figure 5). Thus the stoichiometry of the complex was determined as porphyrin/guest = 1:2. Such phenomena were also observed for 4′,6-diamidino-2-phenylindole (**G6**) and 1-aminomethylpyrene (**G7**).

Figure 6 shows the fluorescence of **G5** (47 nM) versus the concentration of **1**, and the quenching is visible even at a nanomolar concentration of **1**. The binding constants are determined by least-squares-curve fitting of quenching behavior to the 1:1 and 1:2 binding isotherm: $K_1 = [\text{P}\cdot\text{G}]/([\text{P}][\text{G}])$ and $K_2 = [\text{P}\cdot\text{G}_2]/([\text{P}\cdot\text{G}][\text{G}])$, see Equations (1) and (2).

$$\text{P} + \text{G} \rightleftharpoons \text{P}\cdot\text{G} \qquad K_1 \tag{1}$$

$$\text{P}\cdot\text{G} + \text{G} \rightleftharpoons \text{P}\cdot\text{G}_2 \qquad K_2 \tag{2}$$

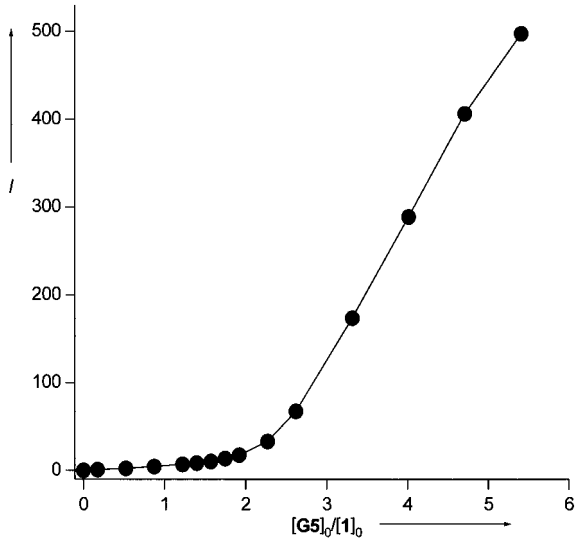

Figure 5. Fluorescence intensity of **G5** in borate buffer ($I = 100$ mM, pH 9.0) at 25 °C in the presence of **1** ($[\mathbf{1}]_0 = 1.2$ μM) versus the concentration of **G5** ($[\mathbf{G5}]_0 = 0-5.4$ μM). Excitation at 490 nm.

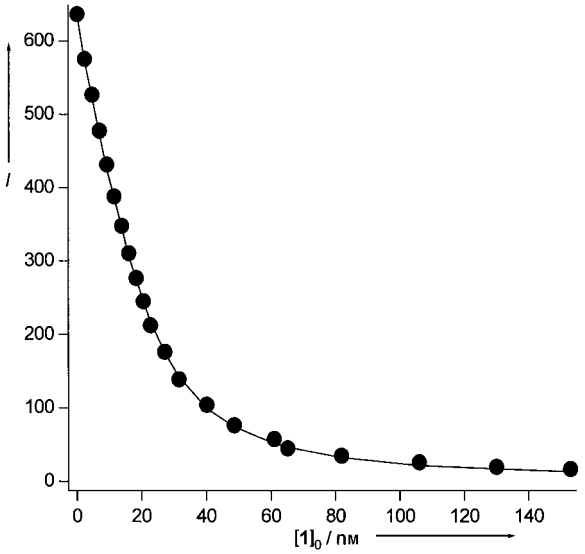

Figure 6. The plot of fluorescence intensity of **G5** (47 nM) against $[\mathbf{1}]_0$ in borate buffer ($I = 100$ mM, pH 9.0) at 25 °C. The simulated curve is also shown.

On the other hand, phenanthidium dyes such as ethidium bromide (**G10**) and propidium iodide (**G11**) exhibit somewhat different spectral changes. Although addition of a guest led to a red-shift of the Soret band in UV-visible titration experiments as shown in Figure 7, the titration curve shows porphyrin/guest = 1:1 complexation. Moreover the fluorescence emission of porphyrin **1** (81 nM) was quenched upon addition of **G11** (Figure 8), here the guest acts as an acceptor for the porphyrin excited state. The binding constants were determined from fluorescence-emission changes of porphyrin by using the 1:1 binding isotherm. For tryptamine (**G8**) and phenethylamine (**G9**), the binding constants were determined by UV-visible titration experiments by using the 1:1 and 1:2 binding isotherm. The results are summarized in Table 1.

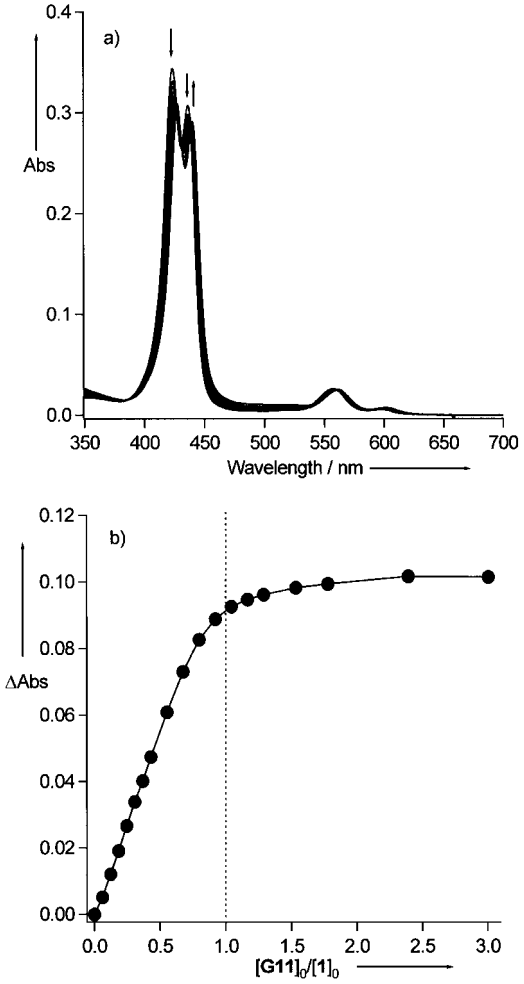

Figure 7. a) UV/Vis spectra of gable porphyrin **1** ($[\mathbf{1}]_0 = 0.63$ μM) titrated with propidium iodide **G11** ($[\mathbf{G11}]_0 = 0-1.9$ μM) in borate buffer ($I =$ 100 mM, pH 9.0) at 25 °C; b) The plot of ΔAbs at 443 nm against $[\mathbf{G11}]_0/[\mathbf{1}]_0$.

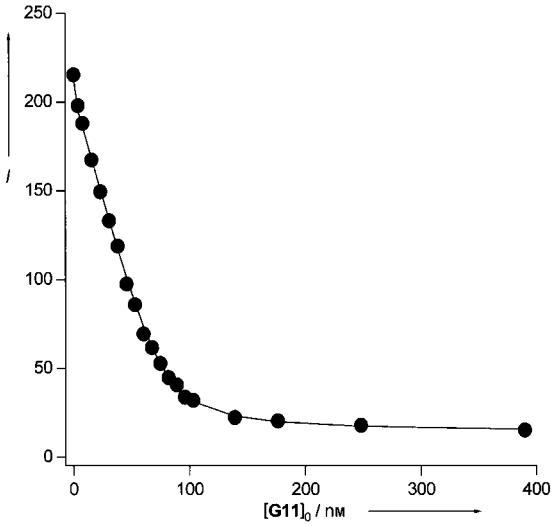

Figure 8. The plot of the fluorescence intensity of **1** (81 nM) at 658 nm in borate buffer ($I = 100$ mM, pH 9.0) at 25 °C against $[\mathbf{G11}]_0$. Excitation at 424 nm. The curve fitted to the 1:1 binding model is also shown.

It should be noted that both the free base $\mathbf{1}\cdot\mathbf{H_2}$ and the zinc complex **1** showed similar affinity for guests **G5**–**G6**; this suggests that coordination to zinc is *not* necessary to bind the DNA intercalators. For the binding of the DNA intercalator, in place of a coordinative interaction, the charge-transfer interaction is important as an additional driving force (vide infra).

Figure 9 shows the fluorescence of **G7** (77 nM), quenched by **1** (745 nM), was recovered up to 70% by the addition of excess diamine **G2** (143 mM). It demonstrates that **G7** binds reversibly and competitively at the gabled cavity of **1** as well as diamine, where pyrene moieties of **G7** are presumably dimerized. According to this binding model, the excimer emission would also be quenched.

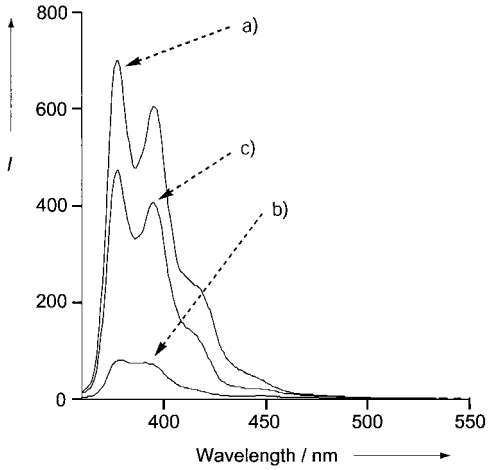

Figure 9. The fluorescence spectra of **G7** (77 nM) in borate buffer (I = 100 mM, pH 9.0) at 25°C. Excitation at 342 nm. a) **G7** only; b) **G7** and **1** (745 nM); c) **G7**, **1**, and diamine **G2** (143 mM).

The following observations suggest that hydrophobic interactions provided by the alkyl chains play an important role: 1) Receptor **1**, with more alkyl groups than **2**, showed larger binding constants for all intercalators, as was observed for diamines. 2) Fluorescence quenching of **G5** by a monomeric analogue **3** provided the value of K_1K_2 of $2.4\times10^{11}\,\mathrm{M}^{-2}$ as the overall binding constant for 1:2 complex formation, indicating that the values of K_1K_2 for the gable porphyrins are 4–5 orders of magnitude larger. 3) The affinity of **G5** for **1** was nearly diminished in MeOH/borate (9:1, *v*/*v*): no UV-visible spectral change was observed upon addition of 5 μM of **G5** to 0.23 μM of **1**. All these findings show that the bound DNA intercalators are stabilized by a large number of alkyl groups of the receptor through hydrophobic interactions.

Guest selectivity and driving forces of binding: The binding constants of **1** increased in the order, **G9** < **G8** < **G7**; this indicates that a larger aromatic system in the guest is favored. Interestingly aliphatic cationic guests such as butylammonium or *N*, *N*, *N*-trimethyl-2-adamantylammonium were not bound to **1**. This is in contrast to the binding behavior of cyclodextrins and cyclophanes, which bind both aromatic and aliphatic guest molecules.[31] Significant spectral changes in the Soret band of gable porphyrins upon binding (Figures 4a and 7a) indicate that there are some perturbations to the porphyrin's electronic states caused by the interaction with the aromatic moiety of the guest. All the guests of intercalator type **G5**–**G11** caused a very similar red-shift in the Soret band in spite of having different binding affinities. It is well known empirically that porphyrin–guest π–π interactions induced a red-shift[32] or hypochromicity[33] of the Soret band. Since both aromatic systems of porphyrin[34] and intercalators[35] have very large polarizability, London dispersion forces must be one of the major driving forces stabilizing the complex. Figure 10 shows the plot of the binding free-energy change, $-\Delta G^\circ$, against the reciprocal of energy differences between the HOMO of the porphyrin and the LUMO of the guests, estimated from semiempirical molecular-orbital calculations based on the PM3-COSMO aqueous solvation model.[36] The guest having a low LUMO level is bound tightly. The linear correlation[37] implies that the charge-transfer interaction between the HOMO of the porphyrin and the LUMO of the guest makes a significant contribution to complex stabilization.

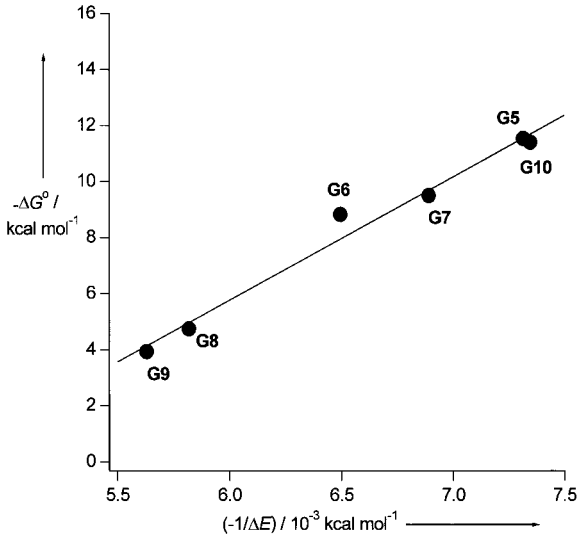

Figure 10. The plots of $-\Delta G^\circ$ for **1**–guest complexation against a reciprocal of energy differences (ΔE) between the HOMO of Zn porphyrin and the LUMO of guests. The least-squares line with $R^2 = 0.982$ is also shown.

Conformational energy as a driving force: Porphyrin receptors show high affinity for cationic aromatic guests, while no affinity for simple cationic guests (e.g. butylammonium), neutral aromatic guest (acridine), or anionic aromatic guest (acridine-9-carboxylate). This trend is associated with the critical balance between electrostatic interaction and hydrophobic interaction on complexation. We suggest that the strict selectivity discriminating the hydrophobicity and charge of guest originates from conformational strain and conformational flexibility of the porphyrins. Without a guest, the folded form of **1** with aggregated hydrophobic moiety is favored due to the hydrophobic stabilization of alkyl–alkyl and alkyl–porphyrin interactions, but unstable due to anion–anion repulsion of the carboxylate groups (folded form, Figure 11). On the other hand, the extended form in which terminal carboxylates are arranged as far apart as possible to minimize

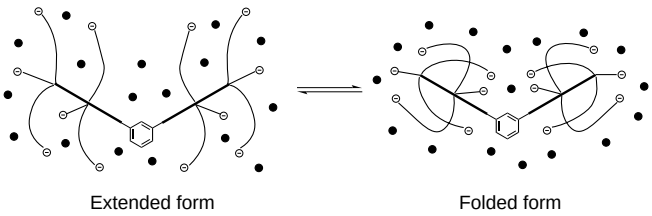

Figure 11. Schematic representation of two extreme conformers of **1** and **2**. In the extended form, due to the repulsion of carboxylate anions the alkyl groups take an extended conformation, and water molecules (●) come into the hydrophobic pocket, destabilizing the conformer. In the folded form, water molecules are expelled so as to have hydrophobic stabilization, but the repulsion between the carboxylate anions destabilizes the conformer.

the electrostatic repulsions, is also unstable due to exposure of the alkyl groups and the porphyrin plane to water (extended form, Figure 11). In either conformation, the hydrophobic interaction and electrostatic interaction cannot both be favorable at the same time; this leads to the destabilization of the initial state of complexation. According to this model, the flexibility of the alkyl chains affects not only the stabilization of the complex but also the destabilization of the guest-free receptor. The binding of hydrophobic cations only can relieve unfavorable conformational stresses and produce larger binding free energies.

Some interesting insight into the conformational instability was obtained by molecular dynamic simulation in the gas phase by using CAChe-augmented MM2 force field parameters with electrostatic interactions incorporated by using a partial charge model. As shown in Figure 12, receptor **1** with 18 carboxylate groups has a larger molecular surface area than the fully protonated **1**; this indicates that the electrostatic repulsion between the carboxylate groups led to a more open (extended) conformation in the gas phase. In water, however, this open conformation should be destabilized due to the larger solvent-accessible area and thus unfavorable hydrophobic interaction, while the folded conformation should be stabilized. Although the relative energy of these two conformers in water is not known, we can expect that these two factors, hydrophobic interactions and electrostatic interactions, operate competitively to determine the actual conformation in water.

Ionic-strength dependence: The contribution of electrostatic interactions to binding was studied in several literature reports.[3c,e, 38] We observed that the binding affinity of DNA intercalators was reduced when the ionic strength I was increased in the range from 0.02–0.5 M (Figure 13). These results suggest the possible role of the carboxylate groups of the receptor in binding as the electrostatic interaction site. The plots of $(\frac{1}{2})\log(K_1K_2)$ (or $\log K_1$) against the square root of ionic strength exhibit a good linear correlation. The Debye–Hückel limiting law gives the relationship between the binding constant and the ionic strength as

$$\frac{1}{2}\log(K_1K_2) = aI^{1/2} + \frac{1}{2}\log(K_{01}K_{02})$$

or

$$\log K_1 = aI^{1/2} + \log K_{01}$$

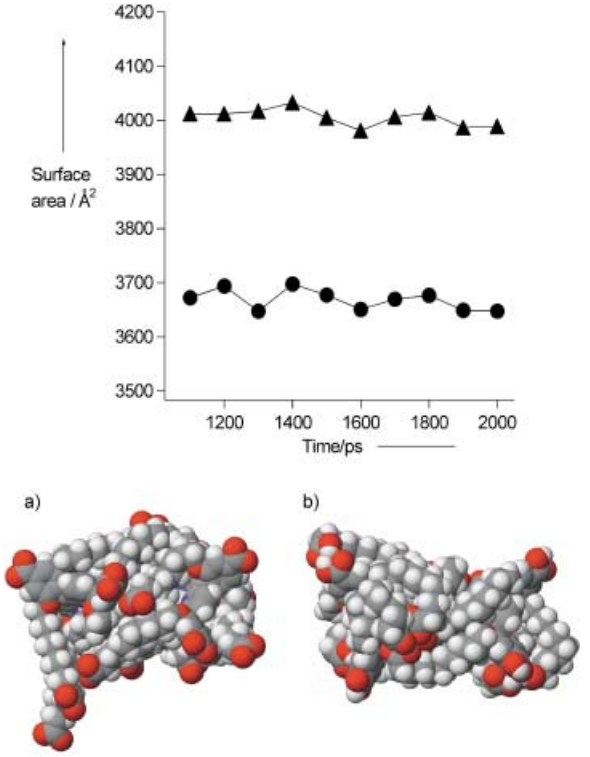

Figure 12. Top: molecular surface area versus simulation time in the molecular dynamic simulation of tetradecaanionic **1** (▲) and fully protonated neutral **1** (●) in vacuo. After the molecule is equilibrated at 500 K for 3000 ps (1 fs per step), molecular dynamic simulation was performed at 300 K for 2000 ps, by using CAChe-augmented MM2 force field parameters. Bottom: snapshot of the 1100 ps frame from the molecular dynamic simulation of a) dodecaanionic **1** and b) protonated neutral **1**, indicating that dodecaanionic **1** tends to take an extended conformation and neutral **1** a folded conformation.

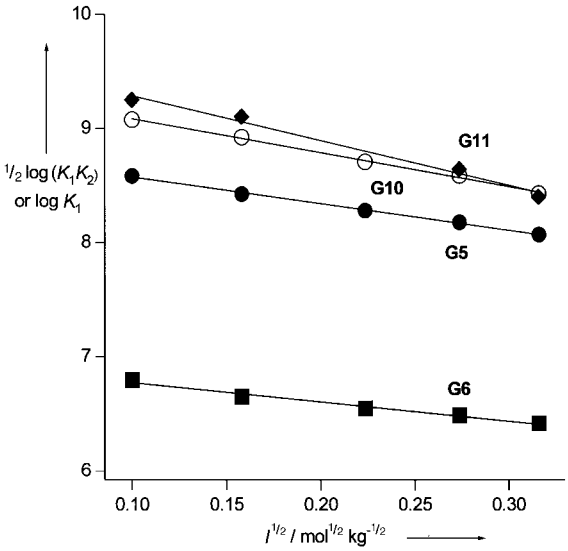

Figure 13. Plot of $\frac{1}{2}\log K_1K_2$ or $\log K_1$ of **1** against the square root of ionic strength ($I^{1/2}$) for **G5** (●), **G6** (■), **G10** (○), and **G11** (◆).

here K_{01} and K_{02} are the binding constants at $I = 0$. For the association between two simple ions with charge z_A and z_B, $a = 1.018\, z_A z_B$ in water at 298 K. The line fitting gives $a = -2.33$, -1.69, -3.92, and -2.97, and $\frac{1}{2}\log(K_{01}K_{02})$, or

$\log K_{01}$, = 8.81, 6.94, 9.68, and 9.38 for **G5**, **G6**, **G10**, and **G11**, respectively. Considering that **1** is a polyanion, the slope a is much smaller than expected from the Debye–Hückel limiting law. This may be ascribed to an interaction mode in which only one to four carboxylates of **1** participate in a salt-bridge with the cationic guest.

Interestingly, the slope a observed for **1** is, except for **G10**, lower than that observed for the binding of basic amino acid derivative, Arg-OMe, to monomeric analogue **3** ($a = -3.08$), which was reported in our previous work.[19] Furthermore, there is no correlation between the number of charges on the guest and slope a. For instance, monocation (**G10**) and dication (**G11**) showed similar a. An explanation for these curious trends remains to be found.

Thermodynamic parameters and enthalpy–entropy compensation: Enthalpy and entropy changes in binding of various guests to **1** in borate buffer were determined by van't Hoff analysis of the binding constants in the temperature range 283–333 K (Table 2). Except for **G8**, the binding was characterized by negative enthalpy changes. The major contributor to the negative enthalpy changes for the binding of diamines was the coordination interaction, and for the binding of DNA intercalators was the charge-transfer interactions. Entropy changes are from -7 to 17 cal K^{-1} mol^{-1}. These values are in contrast to the large negative entropy changes observed for the binding of guest in organic solvents.[19, 25g, 39] The positive entropy changes observed for some of the guests demonstrate that there is significant desolvation. A plot of $T\Delta S^\circ$ against ΔH° for these equilibria gives a linear relationship, $T\Delta S^\circ = \alpha\Delta H^\circ + \beta$ ($\alpha = 0.74$, $\beta =$ 7.75 kcal mol^{-1}); this shows an enthalpy–entropy compensation[40] in this system (Figure 14). Surprisingly, both diamines (**G1**, **G2**, **G4**) and DNA intercalators (**G5**–**8**, **G10**–**11**) are on the same compensation line, in spite of the different binding mechanisms: diamines bind only to the zinc porphyrins (**1** and **2**) while DNA intercalators bind both to the zinc porphyrins and the zinc-free porphyrin (**1**·H_2). This result, that the equilibria with different mechanisms exhibit $\Delta H^\circ - T\Delta S^\circ$ data on the same compensation line, seems contradictory. We would suggest that even for the binding of diamines, desolvation makes significant contributions in addition to the direct zinc–nitrogen interaction.

Table 2. Enthalpy changes (ΔH°) and entropy changes (ΔS°) in binding of guests by zinc gable porphyrin receptor **1** in borate buffer ($I = 100$ mM, pH 9.0).[a]

guest	ΔH° [kcal mol^{-1}]	ΔS° [cal K^{-1} mol^{-1}]
G1	−10.3	0.22
G2	−7.67	4.97
G4	−6.73	5.25
G5	−12.8	−6.40
G6	−3.75	16.9
G7	−6.57	10.1
G8	16.3	66.9
G10	−11.9	−1.19
G11	−12.9	−4.41

[a] ΔH° and ΔS° were determined by fitting binding constants to either $\ln K_1 = -(1/RT)\Delta H^\circ + (1/R)\Delta S^\circ$ for **G1**, **G2**, **G4**, **G10**, and **G11** or $\frac{1}{2}\ln(K_1K_2) = -(1/RT)\Delta H^\circ + (1/R)\Delta S^\circ$ for **G5**–**G8** in the range $283 < T < 333$ K, over which the plot was linear.

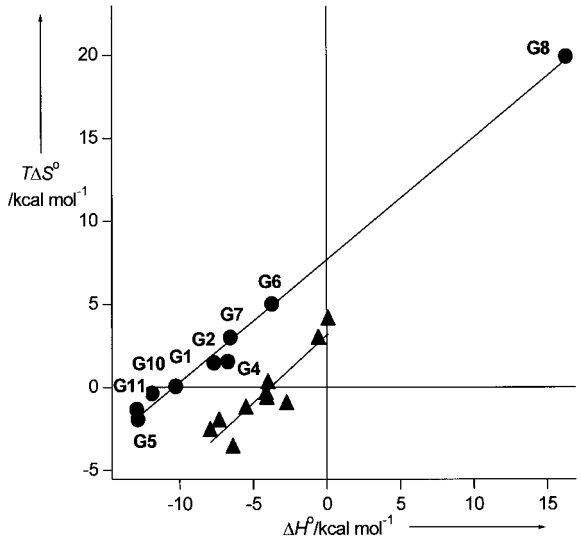

Figure 14. ΔH° versus $T\Delta S^\circ$ compensation plots of **1**–DNA intercalator and **1**–diamine binding (●). $T = 293$ K. The correlation coefficient (r^2) is 0.993. For comparison, ΔH° versus $T\Delta S^\circ$ plots of **3**–amino acid derivatives are also shown (▲).

In Table 3, the slope and the intercept in the ΔH° versus $T\Delta S^\circ$ plots are compared with other representative host–guest systems. According to Inoue et al.[31] the slope (α) reflects the amount of conformational reorganization the host undergoes upon binding. The value of 0.74 is similar to that of cyclophane (0.78) and lower than that of cyclodextrin (0.9).[40] The intercept (β) is associated with the degree of desolvation upon binding. The intercept values of cyclodextrin and cyclophane are 3.1 and 3.4 kcal mol^{-1}, respectively.[40] The large intercept of **1**, 7.75 kcal mol^{-1}, is unprecedented in any artificial host–guest system; this indicates that a considerable desolvation takes place upon binding in our system. Davis and Teague[12] pointed out that induced-fit binding of ligands or drugs to proteins is most frequently driven by hydrophobic contacts with guest rather than by polar interactions, and leads to the hydrophobic collapse of receptors around ligands. In our system also, the guest-induced conformational changes of alkyl moieties provide a larger hydrophobic contact area in the complex as a result of the desolvation of hydrating water molecules around the hydrophobic alkyl groups. It is worthwhile to argue the difference between **1** and monomeric analogue **3** in order to understand fundamental propensity of

Table 3. Slope (α) and intercept (β) in the ΔH° versus $T\Delta S^\circ$ plots for guest binding equilibria of various receptors.

Host	Slope (α)	Intercept (β) [kcal mol^{-1}]	Ref.
1	0.74	7.7	This work
3	0.81	3.1	19
cyclodextrin	0.9	3.1	40
cyclophane/calixarene	0.78	3.4	31
crown ether	0.76	2.4	41
cryptand	0.51	4.0	41

flexible dimeric structure. Although the slope of **1** ($\alpha = 0.74$) is smaller than that of **3** ($\alpha = 0.81$),[19] the intercept of **1** ($\beta =$ 7.7 kcal mol^{-1}) is much larger than that of **3** ($\beta =$ 3.1 kcal mol^{-1}). The intercept reflects the larger size of the gabled binding cavity where the hydrophobicity is effectively enhanced. Such modification by synthetic chemistry has rarely been found in artificial receptors.

Table 3 also compares the slope and the intercept in the ΔH° versus $T\Delta S^\circ$ plots for typical ionophores of crown ether and cryptand. It is apparent that a highly preorganized host such as a cryptand is characterized by a small slope (high compensation temperature) owing to the rigidity of host structure. A similar strategy was also seen in antibody–antigen complexes. Wedmeyer et al.[42] showed that, in the evolution of germline of antibodies by somatic mutation, the matured antibody undergoes very little conformational change between the bound and unbound form, confirming the lock-and-key-type rigid binding. On the other hand, enzymes and signal receptors have flexible binding cavities and conformational diversity,[43] so ligand-induced conformational changes are essential for catalytic action or signal transduction.[44] The artificial receptors of induced-fit type have the capability of responding to external physical or chemical stimuli[45] whereas receptors of the lock-and-key-type, which have a rigid framework, seem to have limited capability. It should be noted again that our system is characterized by a large intercept and a relatively large slope; this indicates that the binding is accompanied by a high degree of reorganization of solvent and moderate reorganization of conformation of the receptor. This study is indicative of the possibility of flexible receptor fabrication to enhance the binding affinity, and gives new insights into the rational design of highly functionalized induced-fit-type water-soluble receptors.

Competitive binding to DNA intercalator with DNA: It is well known that the fluorescence emission of the phenanthidium dyes (**G10** and **G11**) is strikingly enhanced when intercalated into a double helix of DNA.[46] We performed the competitive binding experiment with salmon sperm DNA, **G11**, and receptor **1** in a borate buffer at pH 8 and 9 ([DNA] = 8 μg L^{-1}, [**G11**] = 0.67 μM, [**1**] = 0–0.8 μM). The fluorescence emission of the **G11**–DNA complex was quenched by the addition of **1**, as shown in Figure 15. Concomitantly, a red-shift of the Soret band of **1** in the UV-visible spectrum was observed. The emission spectra were very little affected by the addition of 1.8 μM of Zn-TCPP ([5,10,15,20-tetrakis(4-carboxyphenyl)porphyrinato]zinc) or 3 μM of **3**. This is the first example where intercalator **G11** is transferred from DNA to a synthetic receptor in water.

Conclusion

We have shown that water-soluble gable porphyrin receptors bind tightly to diamines and DNA intercalators where the binding is driven, in general, by hydrophobic interactions. We have further shown that this happens in particular by coordinative interaction in the former guest and by the charge-transfer interaction in the latter. The tight binding of

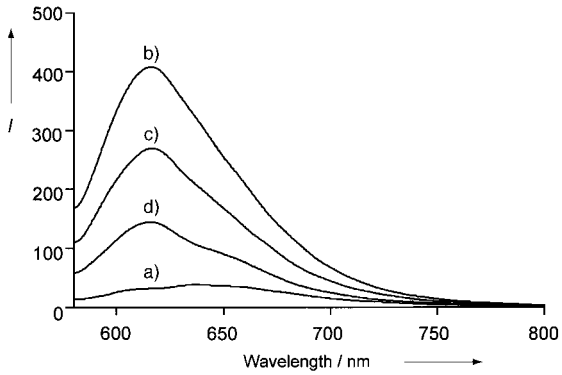

Figure 15. The competitive binding experiment of salmon sperm DNA, DNA intercalator **G11**, and receptor **1** in borate buffer ($I = 100$ mM, pH 9.0) at 25 °C. The fluorescence spectral changes of **G11** are shown. a) **G11** only (0.67 μM); b) **G11** and DNA (8 μg L^{-}); c) **G11**, DNA, and **1** (0.5 μM); d) **G11**, DNA, and **1** (0.8 μM).

DNA intercalators was explained by the unstable conformation of the ω-carboxylatoalkyl groups in the guest-free receptor due to electrostatic repulsion and exposure of the hydrophobic surfaces of alkyl groups/porphyrin framework to water. This instability can be relieved by the binding of hydrophobic cationic guest. The large intercept (α) in the enthalpy–entropy compensation plot corroborates the importance of hydrophobic interactions. The β value of 7.7 kcal mol^{-1} is unprecedented in the binding exhibited by artificial receptors. The flexible nature of the binding pocket and extensive desolvation upon binding are reminiscent of the binding features of proteins. In that case, both conformational energy and desolvation energy should make a significant contribution to the binding energetics as well as the biological functions such as catalysis and signal transduction. The findings will help to understand the biological recognition processes and provide a valuable insight into the rational design of highly-functionalized induced-fit type water-soluble receptors.

Experimental Section

General Methods: ^{1}H NMR spectra were obtained by using a JEOL A-500 spectrometer and chemical shifts are reported relative to Me_4Si or residual protons of deuterated solvents. UV/Vis spectra and fluorescence spectra were recorded on a Hewlett–Packard 8452 diode array spectrophotometer or a Perkin Elmer LS50B luminescense spectrometer with a thermostated cell compartment, respectively. High-resolution mass spectra were obtained with a JEOL JMS-HX110A mass spectrometer by using 3-nitrobenzyl alcohol as a matrix. Small-angle X-ray scattering experiments were performed according to the published procedure.[47]

Materials: Methyl 4-formyl-3,5-bis(10-methoxycarbonyldecyloxy)benzoate (**4**)[19] and dipyrromethane[48] were prepared according to the literature procedure. 1,2-Dichloroethane was distilled over CaH_2. DMF was distilled over P_2O_5.

Titration experiment: Titration experiments were carried out with the aid of UV/Vis or fluorescence spectrometers in the same manner as reported earlier.[19] Binding constants were evaluated by a nonlinear least-squares parameter estimation based on the Damping Gauss–Newton algorithm or the Marquardt algorithm.

5,10,15-Tri[4-methoxycarbonyl-2,6-bis(10-methoxycarbonyldecyloxy)phenyl]porphyrin (5): Aldehyde **4** (1.90 g, 3.2 mmol), pyrrole (152 μL, 2.2 mmol), and dipyrromethane (146 mg, 1.0 mmol) were dissolved in

CH_2Cl_2 (100 mL) under N_2 and then TFA (149 μL, 2.0 mmol) was added. After the solution had stirred at room temperature for 3 h, 2,3-dichloro-5,6-dicyanobenzoquinone (510 mg, 2.2 mmol) was added and the mixture heated under reflux for 2 h. The solution was then neutralized by addition of triethylamine (278 μL, 2 mmol) and concentrated. The residue was subjected to column chromatography (SiO_2, $CHCl_3$/AcOEt 100:1–10:1) to separate **5** and **6**, affording **5** as a purple oil (178 mg, yield 9% based on dipyrromethane). ^{1}H NMR ($CDCl_3$): $\delta = -2.89$ (s, 2H; NH), 0.41–0.95 (m, 76H; CH_2), 1.03 (quin, $J = 7.5$ Hz, 8H; CH_2), 1.34 (quin, $J = 7.5$ Hz, 4H; CH_2), 1.45 (quin, $J = 7.5$ Hz, 8H; CH_2), 2.12 (t, $J = 7.5$ Hz, 4H; CH_2), 2.18 (t, $J = 7.5$ Hz, 8H; CH_2), 3.60 (s, 6H; CO_2Me), 3.61 (s, 12H; CO_2Me), 3.80–3.88 (m, 12H; CH_2), 4.07 (s, 3H; CO_2Me), 4.09 (s, 6H; CO_2Me), 7.63 (s, 2H; phenyl-H), 7.66 (s, 4H; phenyl-H), 8.65 (AB q, $J = 4.5$ Hz, 4H, β-pyrrole), 8.81 (d, $J = 4.5$ Hz, 2H; β-pyrrole), 9.18 (d, $J = 4.5$ Hz, 2H; β-pyrrole), 10.02 (s, 1H; meso-H); HRMS (FAB): calcd for $C_{116}H_{165}N_4O_{24}$ [MH$^+$]: 1998.1813; found 1998.1874.

5,15-Bis[4-methoxycarbonyl-2,6-bis(10-methoxycarbonyldecyloxy)phenyl]porphyrin (6): Following the procedures described above, the reaction mixture was subjected to column chromatographic separation (SiO_2, $CHCl_3$/AcOEt 100:1–10:1). Thorough washing with methanol afforded **6** as a purple solid (100 mg, yield 13% based on dipyrromethane). ^{1}H NMR ($CDCl_3$): $\delta = -3.06$ (s, 2H; NH), 0.38–0.52 (m, 24H; CH_2), 0.61 (quin, $J =$ 7.5 Hz, 8H; CH_2), 0.80 (quin, $J = 7.5$ Hz, 8H; CH_2), 0.88–0.97 (m, 16H; CH_2), 1.40 (quin, $J = 7.5$ Hz, 8H; CH_2), 2.16 (t, $J = 7.5$ Hz, 8H; CH_2), 3.61 (s, 12H; CO_2Me), 3.90 (t, $J = 6.5$ Hz, 8H; CH_2), 4.12 (s, 6H; CO_2Me), 7.70 (s, 4H; phenyl-H), 8.90 (d, $J = 4.5$ Hz, 4H; β-pyrrole), 9.26 (d, $J = 4.5$ Hz, 4H; β-pyrrole), 10.14 (s, 2H; *meso*-H); HRMS (FAB): calcd for [M^+]: $C_{84}H_{114}N_4O_{16}$ 1434.8229; found 1434.8245.

1,3-Phenylenebis{10,15,20-tri[4-methoxycarbonyl-2,6-bis(10-methoxycarbonyldecyloxy)phenyl]porphyrinato zinc(II)} (7): A solution of **5** (939 mg, 470 μmol) and $Zn(OAc)_2$-saturated methanol (10 mL) in $CHCl_3$ (110 mL) was heated under reflux for 3 h. The purification was carried out in a similar manner to the literature procedure[19] to afford a purple oil of zinc porphyrin (937 mg, 454 μmol). A solution of zinc porphyrin (937 mg, 454 μmol) and pyridine (3 mL) in $CHCl_3$ (200 mL) was stirred in an ice bath, then *N*-bromosuccinimide (89 mg, 500 μmol) was added. After 40 min, fluorescence of porphyrin disappeared, and acetone (20 mL) was added to the solution. Evaporation of the solvent and purification by flash column chromatography (SiO_2, $CHCl_3$/AcOEt 10:1) afforded a purple oil of *meso*-brominated zinc porphyrin (930 mg, 434 μmol). Pinacolborane (535 μL, 3.7 mmol) was added to a solution of brominated zinc porphyrin (930 mg, 434 μmol), triethylamine (1 mL), and $PdCl_2(PPh_3)_2$ (14 mg, 20 μmol) in 1,2-dichloroethane (60 mL) under N_2. After the solution had been stirred for 12 h at 80 °C, the fluorescence was recovered. The reaction mixture was washed with saturated aqueous NaCl (100 mL × 2) and the organic layer was dried over Na_2SO_4. Evaporation of the solvent and purification by flash column chromatography (SiO_2, $CHCl_3$/AcOEt 10:1) afforded a purple oil of 5-(4′,4′,5′,5′-tetramethyl[1′,3′,2′]dioxaborolan-2′-yl)-10,15,20-tri[4-methoxycarbonyl-2,6-bis(10-methoxycarbonyldecyloxy)-phenyl]porphyrinato] zinc(II) (870 mg, 398 μmol, 85% from **5**). ^{1}H NMR ($CDCl_3$): $\delta = 0.36–0.98$ (m, 72H; CH_2), 1.24 (t, $J = 7.0$ Hz, 12H; CH_2), 1.30–1.42 (m, 12H; CH_2), 1.81 (s, 12H; BO–CH_3), 2.12 (t, $J = 7.5$ Hz, 12H; CH_2), 3.57 (s, 12H; CO_2Me), 3.59 (s, 6H; CO_2Me), 3.82 (t, $J = 6.5$ Hz, 12H; CH_2), 4.07 (s, 3H; CO_2Me), 4.09 (s, 6H; CO_2Me), 7.63 (s, 2H; phenyl-H), 7.65 (s, 4H; phenyl-H), 8.72 (AB q, $J = 4.5$ Hz; 4H, β-pyrrole), 8.87 (d, $J =$ 4.5 Hz, 2H; β-pyrrole), 9.78 (d, $J = 4.5$ Hz, 2H; β-pyrrole); HRMS (FAB): calcd for $C_{122}H_{173}BN_4O_{26}Zn$ [M^+]: 2185.1721; found 2185.1704.

A solution of 1,3-diiodobenzene in DMF (23 μmol, 71 mM, 324 μL) was added to a solution of porphyrylboronate (125 mg, 57 μmol), $Pd(PPh_3)_4$ (5 mg, 4.3 μmol) and Cs_2CO_3 (40 mg, 123 μmol) in DMF (1.5 mL) under N_2. After the solution had been stirred for 5 h at 80 °C, ethyl acetate (20 mL) was added. The organic layer was washed with saturated aqueous NaCl (20 mL × 2) and dried over Na_2SO_4. Evaporation of the solvent and purification by flash column chromatography (SiO_2, $CHCl_3$/AcOEt 10:1) followed by preparative layer chromatography (SiO_2, hexane/AcOEt 1:1, ×3) afforded a purple oil of **7** (58 mg, 60%, based on diiodobenzene). ^{1}H NMR ($CDCl_3$): $\delta = 0.30–1.06$ (m, 176H; CH_2), 1.18–1.24 (m, 4H; CH_2), 1.37–1.47 (m, 12H; CH_2), 1.71 (t, $J = 7.5$ Hz, 8H; CH_2), 1.81 (t, $J =$ 7.5 Hz, 4H; CH_2), 2.14–2.18 (m, 12H; CH_2), 3.21 (s, 12H; CO_2Me), 3.26 (s, 6H; CO_2Me), 3.57 (s, 12H; CO_2Me), 3.62 (s, 6H; CO_2Me), 3.67–3.72 (m, 4H; CH_2), 3.80–3.84 (m, 12H; CH_2), 3.91 (t, $J = 7.5$ Hz, 8H; CH_2), 4.07 (s, 6H; CO_2Me), 4.11 (s, 12H; CO_2Me), 7.63 (m, 8H; phenyl-H), 7.69 (m, 4H; phenyl-H), 7.93 (t, $J = 7.5$ Hz, 1H; phenyl-H), 8.40 (dd, $^3J = 7.5$ Hz, $^4J =$ 1.5 Hz, 2H; phenyl-H), 8.70 (AB q, $J = 4.5$ Hz, 8H; β-pyrrole), 8.90 (d, $J =$ 4.5 Hz, 4H; β-pyrrole), 9.24 (br s, 1H; phenyl-H), 9.31 (d, $J = 4.5$ Hz, 4H; β-pyrrole); UV/Vis (CH_2Cl_2): λ_{max} (log ε): 421 (5.72), 434 (5.69), 509 (3.84), 551 (4.66), 591 nm (3.80 mol^{-1} dm^3 cm^{-1}); HRMS (FAB): calcd for $C_{238}H_{326}N_8O_{48}Zn_2$ [M^+]: 4192.1894; found 4192.1897 (the observed isotopic distribution of parent ion envelope matched the simulated spectrum).

1,3-Phenylenebis{10,20-bis[4-methoxycarbonyl-2,6-bis(10-methoxycarbonyldecyloxy)phenyl]porphyrinatozinc(II)} (8): Porphyrin **6** was converted to the corresponding boronate in a similar manner to that described for **7** to afford a purple oil of 5-(4′,4′,5′,5′-tetramethyl[1′,3′,2′]dioxaborolan2′-yl)-10,20-bis[4-methoxycarbonyl-2,6-bis(10-methoxycarbonyldecyloxy)phenyl]porphyrinato]zinc(II) in a yield of 88%. ^{1}H NMR ($CDCl_3$): $\delta = 0.30–0.52$ (m, 24H; CH_2), 0.59 (quin, $J = 7.5$ Hz, 8H; CH_2), 0.76–0.95 (m, 24H; CH_2), 1.38 (quin, $J = 7.5$ Hz, 8H; CH_2), 1.80 (s, 12H; BO–CH_3), 2.13 (quin, $J = 7.5$ Hz, 8H; CH_2), 3.58 (s, 12H; CO_2Me), 3.80–3.91 (m, 8H; CH_2), 4.11 (s, 6H; CO_2Me), 7.69 (s, 4H; phenyl-H), 8.88 (d, $J = 5.0$ Hz, 2H; β-pyrrole), 8.93 (d, $J = 4.5$ Hz, 2H; β-pyrrole), 9.24 (d, $J = 4.5$ Hz, 2H; β-pyrrole), 9.78 (d, $J = 5.0$ Hz, 2H; β-pyrrole), 10.08 (s, 1H; *meso*-H); HRMS (FAB): calcd for $C_{90}H_{123}BN_4O_{18}Zn$ [M^+]: 1622.8215; found 1622.8246.

Compound **8** was prepared from this porphyrylboronate (225 mg, 138 μmol) and 1,3-diiodobenzene (55 μmol) in a similar manner to that described for **7**, affording a purple solid in 50% yield (82 mg, 27 μmol). ^{1}H NMR ($CDCl_3$): $\delta = 0.10–1.02$ (m, 120H; CH_2), 1.39 (quin, $J = 7.5$ Hz, 8H; CH_2), 1,65 (m, 8H; CH_2), 2.12 (t, $J = 7.5$ Hz, 8H; CH_2), 3.23 (s, 12H; CO_2Me), 3.57 (s, 12H; CO_2Me), 3.72–3.76 (m, 4H; CH_2), 3.82–3.87 (m, 4H; CH_2), 3.94 (t, $J = 6.5$ Hz, 8H; CH_2), 4.13 (s, 12H; CO_2Me), 7.66 (s, 4H; phenyl-H), 7.72 (s, 4H; phenyl-H), 7.98 (t, $J = 7.5$ Hz, 1H; phenyl-H), 8.49 (dd, $^3J = 7.5$ Hz, $^4J = 1.5$ Hz, 2H; phenyl-H), 8.92 (d, $J = 4.5$ Hz, 4H; β-pyrrole), 8.96 (d, $J = 4.5$ Hz, 4H; β-pyrrole), 9.17 (s, 1H; phenyl-H), 9.25 (d, $J = 4.5$ Hz, 4H; β-pyrrole), 9.35 (d, $J = 4.5$ Hz, 4H; β-pyrrole), 10.07 (s, 2H; *meso*-H); UV/Vis (CH_2Cl_2): λ_{max} (log ε): 415 (5.75), 425 (5.68), 506 (3.75), 545 (4.63), 580 nm (3.76 mol^{-1} dm^3 cm^{-1}); HRMS (FAB): calcd for $C_{174}H_{226}N_8O_{32}Zn_2$ [M^+]: 3067.4883; found 3067.4886 (the observed isotopic distribution of parent ion envelope matched the simulated spectrum).

Octadecapotassium 1,3-phenylenebis{10,15,20-tri[4-carboxylato-2,6-bis(10-carboxylatodecyloxy)phenyl]porphyrinato zinc(II)} (1): Zinc gable porphyrin **7** (34 mg, 8.1 μmol) was dissolved in a solution prepared by mixing THF (14 mL), methanol (4 mL), and KOH (0.5 M, 10 mL). After being stirred at room temperature for 24 h, the solution was concentrated and passed through Sephadex G-15 followed by lyophilization to afford a pink solid of **1** (26 mg, yield 70%). ^{1}H NMR (CD_3OD): $\delta = 0.20–1.50$ (m, 192H; CH_2), 1.91 (t, $J = 7.5$ Hz, 6H; CH_2), 2.00–2.10 (m, 18H; CH_2), 3.70–3.75 (m, 4H; CH_2), 3.82–3.98 (m, 20H; CH_2), 7.67–7.74 (m, 12H; phenyl-H), 8.04 (t, $J = 7.5$ Hz, 1H; phenyl-H), 8.53 (dd, $^3J = 7.5$ Hz, $^4J = 1.5$ Hz, 2H; phenyl-H), 8.65 (AB q, $J = 4.5$ Hz, 8H; β-pyrrole), 8.83 (d, $J = 4.5$ Hz, 4H; β-pyrrole), 9.24 (m, 5H; β-pyrrole and phenyl-H); UV/Vis (borate buffer, $I = 100$ mM, pH 9.0 at 25 °C): λ_{max} (log ε): 423 (5.74), 436 (5.69), 516 (3.87), 557 (4.63), 598 nm (3.99 mol^{-1} dm^3 cm^{-1}).

Octadecapotassium 1,3-phenylenebis{10,20-bis[4-carboxylato-2,6-bis(10-carboxylatodecyloxy)phenyl]porphyrinato zinc(II)} (2): This compound was prepared from **8** (30 mg) in a similar manner to that for **1**: pink solid, yield 76% (25 mg). ^{1}H NMR (CD_3OD): $\delta = 0.06–1.08$ (m, 120H; CH_2), 1.45 (quin, $J = 7.5$ Hz, 8H; CH_2), 1,78 (t, $J = 7.5$ Hz, 8H; CH_2), 2.10 (t, $J =$ 7.5 Hz, 8H; CH_2), 3.76 (m, 4H; CH_2), 3.83 (m, 4H; CH_2), 3.98 (t, $J = 6.0$ Hz, 8H; CH_2), 7.69 (s, 4H; phenyl-H), 7.75 (s, 4H; phenyl-H), 8.08 (t, $J = 7.5$ Hz, 1H; phenyl-H), 8.59 (d, $J = 8.0$ Hz, 2H; phenyl-H), 8.84 (d, $J = 4.5$ Hz, 4H; β-pyrrole), 8.90 (d, $J = 4.5$ Hz, 4H; β-pyrrole), 9.13 (br s, 1H; phenyl-H), 9.22 (d, $J = 4.5$ Hz, 4H; β-pyrrole), 9.28 (d, $J = 4.5$ Hz, 4H; β-pyrrole), 10.01 (s, 2H; *meso*-H); UV/Vis (borate buffer, $I = 100$ mM, pH 9.0 at 25 °C): λ_{max} (log ε): 416 (5.70), 427 (5.61), 509 (3.78), 551 (4.54), 588 nm (3.81 mol^{-1} dm^3 cm^{-1}).

Octadecapotassium 1,3-phenylenebis{10,15,20-tri[4-carboxylato-2,6-bis(10-carboxylatodecyloxy)phenyl]porphyrin} (1·H$_2$): An aqueous solution HCl (1 M, 5 mL) was poured into a solution of **7** (50 mg, 12 μmol) in CH_2Cl_2 (5 mL), and the mixture was stirred vigorously for 1 h at room temperature. The organic layer was washed with saturated aqueous $NaHCO_3$ (20 mL × 2) and saturated aqueous NaCl (20 mL × 2) and dried over Na_2SO_4 to afford a purple oil of 1,3-phenylenebis{10,15,20tri[4-

methoxycarbonyl-2,6-bis(10-methoxycarbonyldecyloxy)phenyl]porphyrin} (48 mg, quant). ^{1}H NMR ($CDCl_3$): $\delta = -2.59$ (s, 2H; NH), 0.35–1.17 (m, 176H; CH_2), 1.33 (quin, $J = 7.5$ Hz, 4H; CH_2), 1.38–1.49 (m, 12H; CH_2), 1.92 (t, $J = 7.5$ Hz, 8H; CH_2), 2.06 (t, $J = 7.5$ Hz, 4H; CH_2), 2.15–2.19 (m, 12H; CH_2), 3.46 (s, 12H; CO_2Me), 3.48 (s, 6H; CO_2Me), 3.58 (s, 12H; CO_2Me), 3.61 (s, 6H; CO_2Me), 3.69 (m, 4H; CH_2), 3.81 (q, $J = 6.5$ Hz, 12H; CH_2), 3.91 (m, 8H; CH_2), 4.07 (s, 6H; CO_2Me), 4.10 (s, 12H; CO_2Me), 7.61, 7.62 (s, 8H; phenyl-H), 7.68 (s, 4H; phenyl-H), 7.93 (t, $J = 7.5$ Hz, 1H; phenyl-H), 8.40 (dd, $^3J = 7.5$ Hz, $^4J = 1.5$ Hz, 2H; phenyl-H), 8.60 (AB q, $J = 4.5$ Hz, 8H; β-pyrrole), 8.80 (d, $J = 4.5$ Hz, 4H; β-pyrrole), 9.19 (d, $J = 4.5$ Hz, 4H; β-pyrrole), 9.25 (br s, 1H; phenyl-H); LRMS (FAB): calcd for $C_{238}H_{330}N_8O_{48}$ [M^+]: 4068.36; found 4068.60. This compound (20 mg) was converted to **1**·H_2 in a similar manner to that for **1**: purple solid, yield 70% (15 mg). ^{1}H NMR (CD_3OD, 50 °C): $\delta = 0.05$–1.47 (m, 192H; CH_2), 1.79 (t, $J = 7.5$ Hz, 6H; CH_2), 1.97–2.08 (m, 18H; CH_2), 3.73 (m, 4H; CH_2), 3.81–3.98 (m, 20H; CH_2), 7.67–7.74 (m, 12H; phenyl-H), 8.13 (t, $J = 7.5$ Hz, 1H; phenyl-H), 8.58 (dd, $^3J = 7.5$ Hz, $^4J = 1.5$ Hz, 2H; phenyl-H), 8.67 (br s, 8H; β-pyrrole), 8.86 (br s, 4H; β-pyrrole), 9.23 (br s, 5H; β-pyrrole and phenyl-H); UV/Vis (borate buffer, $I = 100$ mM, pH 9.0 at 25 °C): λ_{max} (log ε): 419 (5.63), 430 (5.65), 517 (4.61), 551 (4.15), 592 (4.09), 649 nm (3.70 $mol^{-1}\,dm^3\,cm^{-1}$).

Acknowledgdments

The kind help of Ms. Ushitora and Mr. Kobatake with the mass spectroscopic studies is acknowledged. We thank Dr. Kuroda for help in computer-assisted binding constant determinations. This work was supported by a Grant-in-Aid on Priority Areas from the Ministry of Education, Science, Sports, and Culture, Japan. K.W. acknowledges the Japan Society for the Promotion of Science for financial support (JSPS Research Fellowships for Young Scientists).

[1] a) H.-J. Schneider, A. Yatsimirsky, *Principles and Methods in Supramolecular Chemistry*, Wiley, Chichester, **2000**; b) M. W. Peczuh, A. D. Hamilton, *Chem. Rev.* **2000**, *100*, 2479.

[2] For recent studies on porphyrin receptors see: a) M. Sirish, V. A.Chertkov, H.-J. Schneider, *Chem. Eur. J.* **2002**, *8*, 1181; b) H. Imai, K. Misawa, H. Munakata, Y. Uemori, *Chem. Lett.* **2001**, 688; c) R. K. Jain, A. D. Hamilton, *Org. Lett.* **2000**, *2*, 1721; d) M. Sirish, H.-J. Schneider, *J. Am. Chem. Soc.* **2000**, *122*, 5881; e) M. Sirish, H.-J. Schneider, *Chem. Commun.* **1999**, 907–908.

[3] For recent studies on cyclodextrin receptors see: a) A. Bom, M. Bradley, K. Cameron, J. K. Clark, J. van Egmond, H. Feilden, E. J. MacLean, A. W. Muir, R. Palin, D. C. Rees, M.-Q. Zhang, *Angew. Chem.* **2002**, *114*, 275–280; *Angew. Chem. Int. Ed.* **2002**, *41*, 265; b) J. J. Michels, R. Fiammengo, P. Timmerman, J. Huskens, D. N. Reinhoudt, *J. Inclusion Phenom. Macrocyclic Chem.* **2001**, *41*, 163–172; c) K. Kano, T. Kitae, Y. Shimofuri, N. Tanaka, Y. Mineta, *Chem. Eur. J.* **2000**, *6*, 2705; d) M. Ghosh, R. Zhang, R. G. Lawler, C. T. Seto, *J. Org. Chem.* **2000**, *65*, 735; e) R. Breslow, Z. Yang, R. Ching, G. Trojandt, F. Odobel, *J. Am. Chem. Soc.* **1998**, *120*, 3536; f) T. Kitae, T. Nakayama, K. Kano, *J. Chem. Soc. Perkin Trans. 2* **1998**, 207.

[4] For recent studies on cyclophane receptors see: a) S. Otto, R. L. E. Furlan, J. K. M. Sanders, *Science* **2002**, *297*, 590; b) V. Dvornikovs, D. B. Smithrud, *J. Org. Chem.* **2002**, *67*, 2160; c) S. M. Ngola, P. C. Kearney, S. Mecozzi, K. Russell, D. A. Dougherty, *J. Am. Chem. Soc.* **1999**, *121*, 1192; d) M. Inouye, K. Fujimoto, M. Furusyo, H. Nakazumi, *J. Am. Chem. Soc.* **1999**, *121*, 1452.

[5] For recent studies on other receptors see: a) M. Herm, O. Molt, T. Schrader, *Chem. Eur. J.* **2002**, *8*, 1485; b) F. Corbellini, R. Fiammengo, P. Timmerman, M. Crego-Calama, K. Versluis, A. J. R. Heck, I. Luyten, D. N. Reinhoudt, *J. Am. Chem. Soc.* **2002**, *124*, 6569; c) A. L. Satz, T. C. Bruice, *J. Am. Chem. Soc.* **2001**, *123*, 2469; d) S. Rensing, M. Arendt, A. Springer, T. Grawe, T. Schrader, *J. Org. Chem.* **2001**, *66*, 5814; e) X. Gui, J. C. Sherman, *Chem. Commun.* **2001**, 2680; f) S. L. McKay, B. Haptonstall, S. H. Gellman, *J. Am. Chem. Soc.* **2001**, *123*, 1244; g) T. Lan, L. W. McLaughlin, *J. Am. Chem. Soc.* **2001**, *123*, 2064; h) P. Anzenbacher, Jr., K. Jursikova, J. L. Sessler, *J. Am. Chem. Soc.* **2000**, *122*, 9350; i) R. B. Prince, S. A. Barnes, J. S. Moore, *J. Am. Chem. Soc.* **2000**, *122*, 2758; j) N. Sugimoto, D. Miyoshi, J. Zou, *Chem. Commun.* **2000**, 2295; k) S. Sun, M. A. Fazal, B. C. Roy, S. Mallik, *Org. Lett.* **2000**, *2*, 911; l) E. Kikuta, M. Murata, N. Katsube, T. Koike, E. Kimura, *J. Am. Chem. Soc.* **1999**, *121*, 5426; m) T. Haino, D. M. Rudkevich, J. Rebek, Jr., *J. Am. Chem. Soc.* **1999**, *121*, 11253; n) T. W. Bell, A. B. Khasanov, M. G. B. Drew, A. Filikov, T. L. James, *Angew. Chem.* **1999**, *111*, 2705; *Angew. Chem. Int. Ed.* **1999**, *38*, 2543; o) J. Kawakami, T. Kitano, N. Sugimoto, *Chem. Commun.* **1999**, 1765; p) K. Niikura, A. Metzger, E. V. Anslyn, *J. Am. Chem. Soc.* **1998**, *120*, 8533; q) M. A. Hossain, H.-J. Schneider, *J. Am. Chem. Soc.* **1998**, *120*, 11208; r) M. W. Peczuh, A. D. Hamilton, J. Sánchez-Quesada, J. de Mendoza, T. Haack, E. Giralt, *J. Am. Chem. Soc.* **1997**, *119*, 9327.

[6] I. D. Kuntz, K. Chen, K. A. Sharp, P. A. Kollman, *Proc. Natl. Acad. Sci. USA* **1999**, *96*, 9997.

[7] M. V. Rekharsky, Y. Inoue, *Chem. Rev.* **1998**, *98*, 1875.

[8] M. W. Hosseini, A. J. Blacker, J.-M. Lehn, *J. Am. Chem. Soc.* **1990**, *112*, 3896.

[9] R. Breslow, S. Halfon, B. Zhang, *Tetrahedron* **1995**, *51*, 377.

[10] a) D. J. Cram, *Angew. Chem.* **1986**, *98*, 1041; *Angew. Chem. Int. Ed. Engl.* **1986**, *25*, 1039; b) D. J. Cram, *Science* **1988**, *240*, 760; c) A. E. Martell, R. Hancock, R. J. Motekaitis, *Coord. Chem. Rev.* **1994**, *133*, 39.

[11] P. R. Andrews, D. J. Craik, J. L. Martin, *J. Med. Chem.* **1984**, *27*, 1648.

[12] A. M. Davis, S. J. Teague, *Angew. Chem.* **1999**, *111*, 778; *Angew. Chem. Int. Ed.* **1999**, *38*, 736.

[13] R. K. Jain, A. D. Hamilton, *Angew. Chem.* **2002**, *114*, 663; *Angew. Chem. Int. Ed.* **2002**, *41*, 641; H. S. Park, Q. Lin, A. D. Hamilton, *J. Am. Chem. Soc.* **1999**, *121*, 8.

[14] T. J. Matray, E. T. Kool, *J. Am. Chem. Soc.* **1998**, *120*, 6191.

[15] D. B. Smithrud, F. Diederich, *J. Am. Chem. Soc.* **1990**, *112*, 339.

[16] D. E. Koshland, Jr., *Angew. Chem.* **1994**, *106*, 2468; *Angew. Chem. Int. Ed. Engl.* **1994**, *33*, 2315.

[17] a) I. Tabushi, T. Sasaki, *Tetrahedron Lett.* **1982**, *23*, 1913; b) I. Tabushi, S. Kugimiya, M. G. Kinnaird, T. Sasaki, *J. Am. Chem. Soc.* **1985**, *107*, 4192.

[18] S. Kugimiya, *Chem. Commun.* **1990**, 432.

[19] a) T. Mizutani, K. Wada, S. Kitagawa, *J. Am. Chem. Soc.* **1999**, *121*, 11425; b) T. Mizutani, K. Wada, S. Kitagawa, *J. Org. Chem.* **2000**, *65*, 6097.

[20] J. S. Lindsey in *The Porphyrin Handbook*, *Vol. 1* (Eds.: K. M. Kadish, K. M. Smith, R. Guilard), Academic Press, San Diego, **2000**, pp 45–118.

[21] S. G. DiMagno, V. S. Y. Lin, M. J. Therien, *J. Org. Chem.* **1993**, *58*, 5983.

[22] A. G. Hyslop, M. A. Kellett, P. M. Iovine, M. J. Therien, *J. Am. Chem. Soc.* **1998**, *120*, 12676.

[23] N. Miyaura, A. Suzuki, *Chem. Rev.* **1995**, *95*, 2457.

[24] T. Mizutani, K. Wada, S. Kitagawa, *Chem. Commun.* **2002**, 1626.

[25] a) M. Nappa, J. S. Valentine, *J. Am. Chem. Soc.* **1978**, *100*, 5075; b) C. Verchere-Beaur, E. Mikros, M. Perree-Fauvet, A. Gaudemer, *J. Inorg. Biochem.* **1990**, *40*, 127; c) T. Mizutani, T. Ema, T. Tomita, Y. Kuroda, H. Ogoshi, *J. Am. Chem. Soc.* **1994**, *116*, 4240; d) Y. Kuroda, Y. Kato, T. Higashioji, J. Hasegawa, S. Kawanami, M. Takahashi, N. Shiraishi, K. Tanabe, H. Ogoshi, *J. Am. Chem. Soc.* **1995**, *117*, 10950; e) T. Mizutani, T. Murakami, N. Matsumi, T. Kurahashi, H. Ogoshi, *Chem. Commun.* **1995**, 1257; f) R. P. Bonar-Law, *J. Org. Chem.* **1996**, *61*, 3623; g) T. Mizutani, T. Murakami, T. Kurahashi, H. Ogoshi, *J. Org. Chem.* **1996**, *61*, 539; h) T. Mizutani, T. Kurahashi, T. Murakami, N. Matsumi, H. Ogoshi, *J. Am. Chem. Soc.* **1997**, *119*, 8991.

[26] C. A. Hunter, J. K. Sanders, A. J. Stone, *Chem. Phys.* **1989**, *133*, 395.

[27] M. Kasha, *Radiat. Res.* **1963**, *20*, 55; M. Kasha, H. R. Rawls, M. Ashraf, A. El-Bayoumi, *Pure Appl. Chem.* **1965**, *11*, 371.

[28] a) T. Hayashi, T. Aya, M. Nonoguchi, T. Mizutani, Y. Hisaeda, S. Kitagawa, H. Ogoshi, *Tetrahedron* **2002**, *58*, 2803; b) V. V. Borovkov, J. M. Lintuluoto, Y. Inoue, *Org. Lett.* **2002**, *4*, 169; c) V. V. Borovkov, J. M. Lintuluoto, M. Fujiki, Y. Inoue, *J. Am. Chem. Soc.* **2000**, *122*, 4403; d) M. J. Crossley, T. W. Hambley, L. G. Mackay, A. C. Try, R. Walton, *Chem. Commun.* **1995**, 1077; e) S. Matile, N. Berova, K. Nakanishi, J. Fleischhauer, R. W. Woody, *J. Am. Chem. Soc.* **1996**, *118*, 5198.

[29] a) G. M. Blackburn, M. J. Gait, *Nucleic Acids in Chemistry and Biology*, Oxford University Press, Oxford, **1990**; b) W. Saenger, *Principles of Nucleic-Acid Structure*, Springer, New York, **1984**.
[30] T. Mizutani, K. Wada, S. Kitagawa, *J. Am. Chem. Soc.* **2001**, *123*, 6459.
[31] Y. Inoue, Y. Liu, L.-H. Tong, B.-J. Shen, D.-S. Jin, *J. Am. Chem. Soc.* **1993**, *115*, 10637.
[32] H.-J. Schneider, L. Tianjun, M. Sirish, V. Malinovski, *Tetrahedron* **2002**, *58*, 779.
[33] T. Hayashi, T. Miyahara, N. Koide, Y. Kato, H. Masuda, H. Ogoshi, *J. Am. Chem. Soc.* **1997**, *119*, 7281.
[34] a) K. Kano, H. Minamizono, T. Kitae, S. Negi, *J. Phys. Chem. A* **1997**, *101*, 6118; b) K. Kano, T. Hayakawa, S. Hashimoto, *Bull. Chem. Soc. Jpn.* **1991**, *64*, 778.
[35] D. Reha, M. Kabelac, F. Ryjacek, J. Sponer, J. E. Sponer, M. Elstner, S. Suhai, P. Hobza, *J. Am. Chem. Soc.* **2002**, *124*, 3366.
[36] A. Klamt, G. Schüürmann, *J. Chem. Soc. Perkin Trans. 2* **1993**, 799.
[37] R. S. Mulliken, *J. Am. Chem. Soc.* **1950**, *72*, 600.
[38] a) H.-J. Schneider, R. Kramer, S. Simova, U. Schneider, *J. Am. Chem. Soc.* **1988**, *110*, 6442; b) M. A. Hossain, H.-J. Schneider, *Chem. Eur. J.* **1999**, *5*, 1284; c) T. Mizutani, T. Horiguchi, H. Koyama, I. Uratani, H. Ogoshi, *Bull. Chem. Soc. Jpn.* **1998**, *71*, 413; d) K. O. Lara, C. Godoy-Alcantar, I. L. Rivera, A. V. Eliseev, A. K. Yatsimirsky, *J. Phys. Org. Chem.* **2001**, *14*, 453.
[39] a) H. Ogoshi, T. Mizutani, T. Hayashi, Y. Kuroda in *Handbook of Porphyrins and Related Macrocycles: Biomaterials for Materials Scientist*, *Chemists*, *and Physicists*, *Vol. 6* (Eds.: K. Kadish, K. M. Smith, R. Guillard), Academic Press, San Diego, **2000**, pp 279–340; b) T. Hayashi, T. Miyahara, Y. Aoyama, M. Kobayashi, H. Ogoshi, *Pure Appl. Chem.* **1994**, *66*, 797; c) Y. Kuroda, Y. Kato, T. Higashioji, J. Hasegawa, S. Kawanami, M. Takahashi, N. Shiraishi, K. Tanabe, H. Ogoshi, *J. Am. Chem. Soc.* **1995**, *117*, 10950; d) H. Ogoshi, T. Mizutani, *Acc. Chem. Res.* **1998**, *31*, 81.
[40] a) Y. Inoue, T. Hakushi, Y. Liu, L. Tong, B. Shen, D. Jin, *J. Am. Chem. Soc.* **1993**, *115*, 475; b) M. V. Rekharsky, Y. Inoue, *Chem. Rev.* **1998**, *98*, 1875.
[41] Y. Inoue, T. Hakushi, *J. Chem. Soc. Perkin Trans. 2* **1985**, 935.
[42] G. J. Wedemayer, P. A. Patten, L. H. Wang, P. G. Schultz, R. C. Stevens, *Science* **1997**, *276*, 1665.
[43] H. A. Carlson, J. A. Mccammon, *Mol. Pharmacol.* **2000**, *57*, 213.
[44] a) M. F. Perutz, *Mechanisms of Cooperativity and Allosteric Regulation in Proteins*, Cambridge University Press, Cambridge, **1989**; b) H. Dugas, *Bioorganic Chemistry—A Chemical Approach to Enzyme Action*, *2nd ed.*, Springer, New York, **1989**; c) B. Alberts, D. Bray, J. Lewis, M. Raff, K. Roberts, J. D. Watson, *Molecular Biology of the Cell*, *3rd ed*, Garland, New York, **1994**; d) C. Branden, J. Tooze, *Introduction to Protein Structure*, *2nd ed*, Garland, New York, **1991**.
[45] a) H. L. Anderson, C. A. Hunter, M. N. Meah, J. K. M. Sanders, *J. Am. Chem. Soc.* **1990**, *112*, 5780; b) C.-W. Chen, J. H. W. Whitlock, *J. Am. Chem. Soc.* **1978**, *100*, 4921; c) S. Goswami, D. V. Engen, A. D. Hamilton, *J. Am. Chem. Soc.* **1989**, *111*, 3425; d) A. D. Hamilton, D. V. Engen, *J. Am. Chem. Soc.* **1987**, *109*, 5035; e) M. Inouye, T. Konishi, K. Isagawa, *J. Am. Chem. Soc.* **1993**, *115*, 8091; f) J. Rebek, Jr., B. Askew, P. Ballester, C. Buhr, S. Jones, D. Nemeth, K. Williams, *J. Am. Chem. Soc.* **1987**, *109*, 5033; g) T. Mizutani, N. Sakai, S. Yagi, T. Takagishi, S. Kitagawa, H. Ogoshi, *J. Am. Chem. Soc.* **2000**, *122*, 748; h) T. Mizutani, S. Yagi, A. Honmaru, H. Ogoshi, *J. Am. Chem. Soc.* **1996**, *118*, 5318; i) T. Nabeshima, H. Furusawa, Y. Yano, *Angew. Chem.* **1994**, *106*, 1849; *Angew. Chem. Int. Ed. Engl.* **1994**, *33*, 1750; j) T. Nabeshima, A. Hashiguchi, S. Yazawa, T. Haruyama, Y. Yano, *J. Org. Chem.* **1998**, *63*, 2788; k) H.-J. Schneider, D. Ruf, *Angew. Chem.* **1990**, *102*, 1192; *Angew. Chem. Int. Ed. Engl.* **1990**, *29*, 1159; l) M. Takeuchi, T. Imada, S. Shinkai, *Angew. Chem.* **1998**, *110*, 2242; *Angew. Chem. Int. Ed.* **1998**, *37*, 2096; m) T. Tjivikua, G. Deslongchamps, J. Rebek, Jr., *J. Am. Chem. Soc.* **1990**, *112*, 8408; n) T. G. Traylor, M. J. Mitchell, J. P. Ciccone, S. Nelson, *J. Am. Chem. Soc.* **1982**, *104*, 4986; o) T. Kawabata, M. Nagato, K. Takasu, K. Fuji, *J. Am. Chem. Soc.* **1997**, *119*, 3169; p) Y. Kubo, T. Ohno, J. Yamanaka, S. Tokita, T. Iida, Y. Ishimaru, *J. Am. Chem. Soc.* **2001**, *123*, 12700.
[46] a) J. Olmsted, D. R. Kearns, *Biochemistry* **1977**, *16*, 3647; b) W. D. Wilson, Y. H. Wang, C. R. Krishnamoorthy, J. C. Smith, *Biochemistry* **1985**, *24*, 3991; c) R. L. Jones, G. Zon, C. R. Krishnamoorthy, W. D. Wilson, *Biochemistry* **1986**, *25*, 7431.
[47] N. Ise, T. Okubo, S. Kunugi, H. Matsuoka, K. Yamamoto, Y. Ishii, *J. Chem. Phys.* **1984**, *81*, 3294.
[48] B. J. Littler, M. A. Miller, C.-H. Hung, R. W. Wagner, D. F. O'Shea, P. D. Boyle, J. S. Lindsey, *J. Org. Chem.* **1999**, *64*, 1391.

Received: October 7, 2002 [F4481]